Electronics Supplementary Information

Rational design and controllable preparation of holey MnO_2 nanosheets

Gaini Zhang, Lijun Ren, Zhe Yan, Liping Kang, Zhibin Lei, Hua Xu, Feng Shi,

*Zong-Huai Liu**

Key Laboratory of Applied Surface and Colloid Chemistry (Shaanxi Normal University), Ministry of Education, Xi'an 710062, China, School of Materials Science and Engineering, Shaanxi Normal University, Xi'an 710062, China.

*Corresponding Author: Zong-Huai Liu

E-mail: zhliu@snnu.edu.cn

Experimental Section

Tetramethylammonium hydroxide solution (TMAOH, 25 wt.%, analytical grade) was purchased from Alfa Aesar Co., others chemicals used in this work were analytical grade, commercially available from Sinopharm Chemical reagent Co., Ltd. China, and used without further purification. All solutions were prepared using ultrapure water (resistance > 18.2 MΩ cm^{-1}).

1. Preparation of MnO_2 Nanosheets: The MnO_2 nanosheets were prepared according to the previous report with some modification.[1] A mixed solution of 30 % H_2O_2 and 0.6 mol L^{-1} TMAOH was quickly added to 0.3 mol L^{-1} $MnCl_2 \cdot 4H_2O$ aqueous solution under vigorously stirring at room temperature. The reaction was completed immediately, and a dark-brown

suspension was obtained. The resulting suspension was stirred vigorously overnight, centrifuged at a speed of 8000 rpm for 15 min, and dialyzed until the pH was 7. The MnO_2 nanosheets slurry was obtained, which contained well-dispersed MnO_2 nanosheets. After it was freeze-drying for 12 h, the assembled materials by MnO_2 nanosheets were finally prepared, and denoted as MnO_2-0.

2. Preparation of Holey MnO_2 Nanosheets: The MnO_2 nanosheets suspension (3.48 mL, 5 mg mL^{-1}) and excess copper wire were added to 200 mL of aqueous solution containing 7.5 mmol L^{-1} HCl and 0.25 mmol L^{-1} $FeCl_3 \cdot 6H_2O$, simultaneously. After treating by different times (3 h, 6 h, and 9 h), the copper wire was picked out, and the obtained product was washed by vacuum filtration with ultrapure water for several times. Then, it was re-dispersed in a 0.1 mol L^{-1} HCl solution at room temperature for 12 h to remove metal-containing species, such as metal ions and metal oxides, and rinsed with deionized water, again, the holey MnO_2 nanosheets suspension was obtained. By freeze-drying the holey MnO_2 nanosheets suspension for 12 h, the assembled materials by holey MnO_2 nanosheets were finally prepared, which were denoted as MnO_2-*x*, where *x* represented the holey treatment time.

Via a double dripping mode, MnO_2 nanosheets suspension (0.087 mg mL^{-1}, 200 mL) and $FeCl_2 \cdot 6H_2O$ solution (0.1 mmol L^{-1}, 200 mL) containing 15 mmol L^{-1} HCl are softly added into a reaction vessel with an equal volume and the mixed suspension is stirred for 6 h at room temperature, FeO_x/MnO_2 intermediate product was obtained. Then it was immersed in 0.1 mol L^{-1} HCl solution and stirred for 12 h at room temperature, FeO_x was etched and MnO_2 sample was obtained.

3. Structural Characterization

The crystal structure of the samples was examined using X-ray diffractometry (XRD, D/Max2550VB+/PC) with Cu Kα radiation in the range from 5 to 70° with a step size of 5°/min. The microstructure of the samples was observed by transmission electron microscopy (TEM, JEM-2010) at an acceleration voltage of 200 kV. The thickness of the MnO_2 nanosheets was examined using atomic force microscopy (AFM, Bruker Dimension ICON). The suspension of the obtained MnO_2 nanosheets were spin coated on mica substrates by spin coater (KW-4B, Institute of microelectronics, Chinese academy of sciences) operating at 500 revolution/min for 60 s. The Nitrogen adsorption/desorption isotherms were measured at 77 K on ASAP 2420 analyzer. Prior to analysis, all samples were degassed under vacuum at 120 °C for at least 12 h. The specific surface area was calculated using the Brunauer-Emmett-Teller (BET) method with the adsorption data at the relative pressure (P/P_0) range of 0.05-0.20. The total pore volume was estimated at P/P_0=0.99. The pore size distribution was determined from adsorption branch using the nonlocal density functional theory (NLDFT) model assuming the slit pore geometry. X-ray photoelectron spectroscopy (XPS) spectra were collected on an AXIS ULTRA spectrometer (Kratos Analytical) with an Al Kα X-ray source (1468.71 eV). All binding energies were calibrated using carbon C1s peak at 284.6 eV as a reference.

4. Electrochemical Characterization

The electrochemical performances of the electrode materials in 1.0 mol L^{-1} Na_2SO_4 aqueous electrolyte were characterized by cyclic voltammetry, galvanostatic charge-discharge and electrochemical impedance spectrocopy on IVIUMSTAT electrochemical

workstation (Ivium Technologies BV Co., Holland). The working electrode was prepared by mixing an active material (75 wt.%) with carbon black (20 wt.%) as the conducting material and polytetrafluoroethylene (PTFE, 5 wt.%) as the binder in water. The slurry of the mixture was then pasted between two pieces of Ni foam (1.2 cm^2) as the current collector and pressed under a pressure of 100 kg cm^{-2}. The resultant electrodes were dries in an oven at 100 °C for 6 h. The mass loading for each electrode is about 2.5 mg cm^{-2}. The electrochemical test of the electrode was performed in a conventional three-electrode system, in which Pt foil and saturated calomel electrode (SCE) were applied as counter and reference electrodes, respectively. The specific capacitance (C, F g^{-1}) of the electrode materials was calculated from the galvanostatic discharge process according to the following equation: $C = I \times \Delta t /(m \times \Delta V)$, where I, Δt, m, and ΔV represent the discharge current, discharge time, mass of the active material and voltage change excluding the IR drop during the discharge process, respectively.

In a two-electrode cell, symmetric supercapacitors MnO_2-6//MnO_2-6 and MnO_2-0//MnO_2-0 were fabricated via assembly of two pieces of identical working electrodes and a piece of separator (Whatman 1820). 1.0 mol L^{-1} Na_2SO_4 aqueous was used as electrolyte. The ion kinetics within an electrode material is investigated by electrochemical impedance spectroscopy (EIS) at the frequency range of 0.005 Hz to 100 kHz with on CHI660E electrochemical workstation (CH Instruments Inc. China).

Supplementary Figures

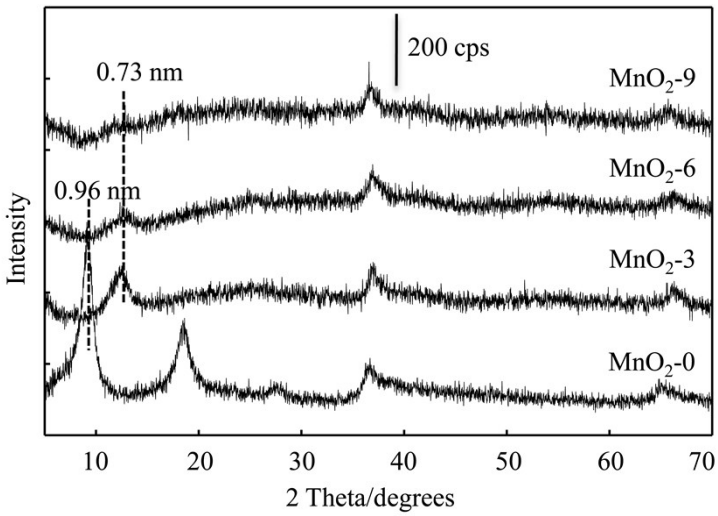

Fig. S1 XRD patterns of the assembled materials by holey MnO_2 nanosheets with different treatment times.

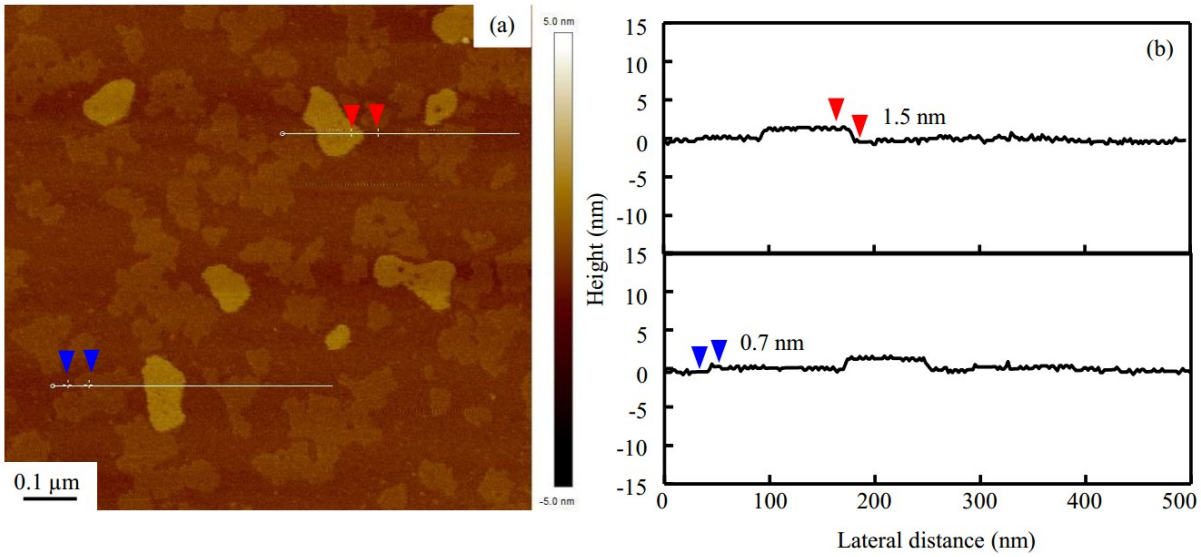

Fig. S2 AFM image of the MnO_2 nanosheets on mica substrate (a) and the height difference between two blue/red arrows is 0.7/1.5 nm (b).

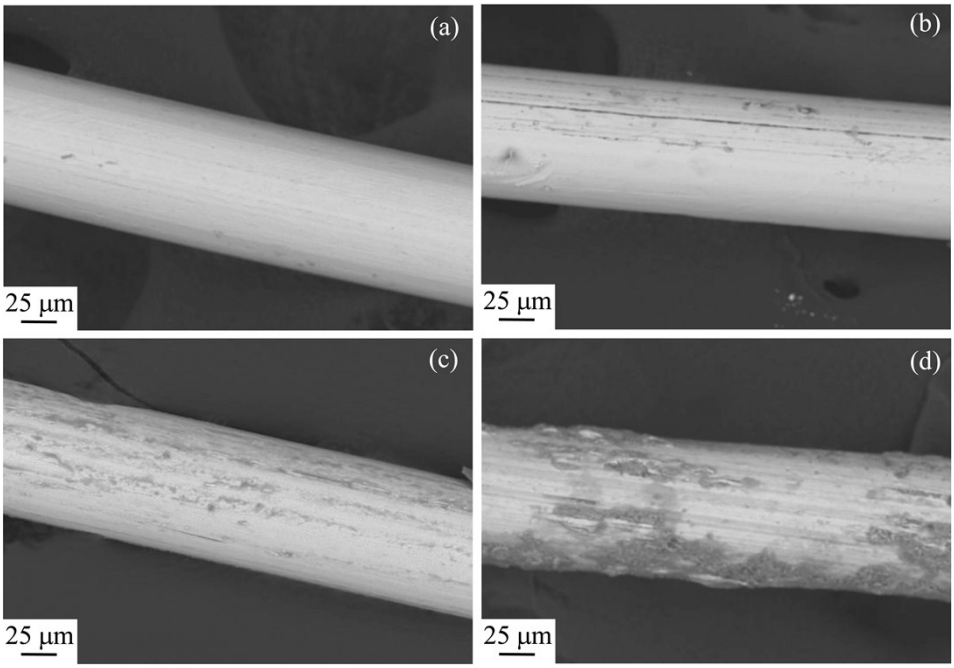

Fig. S3 SEM images of Cu wires with different treatment times: (a) 0 h, (b) 3 h, (c) 6 h, and (d) 9 h, respectively.

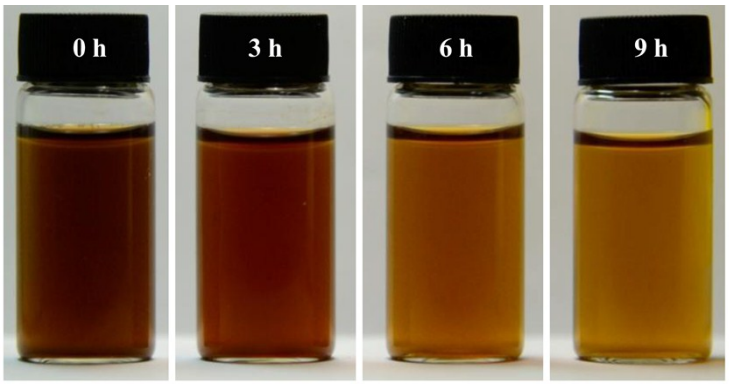

Fig. S4 Digital photographs of the suspension with different treatment times.

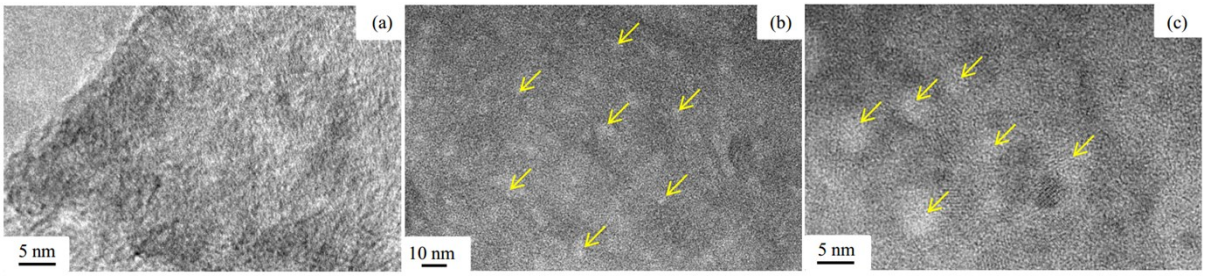

Fig. S5 HR-TEM images of the MnO_2 nanosheets (a) and holey MnO_2-6 nanosheets with different magnifications (b, c).

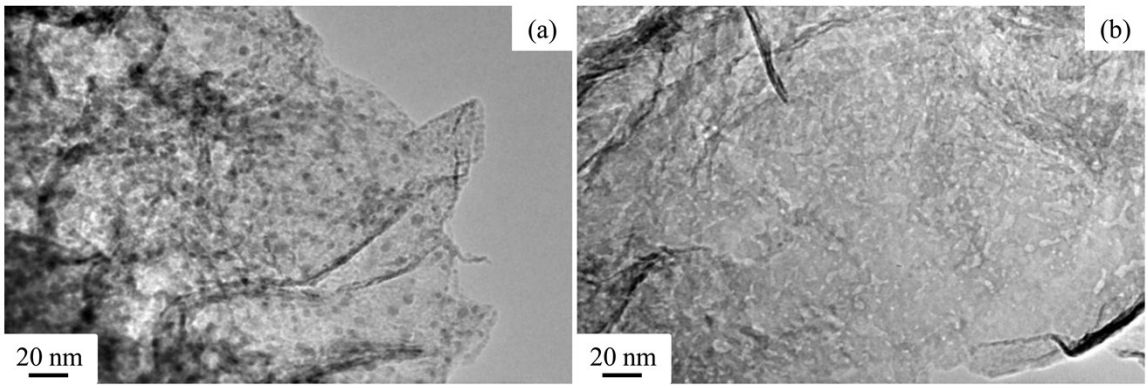

Fig. S6 TEM images of the intermediate product FeO_x/MnO_2 before (a) and after (b) treated with HCl solution.

Table S1 Comparative synthesis method, types of pore and specific surface area of porous MnO_2 materials reported by the literatures

Samples	**Synthesis methods**	**Types of pore[a]**	**S_{BET}[b] ($m^2\ g^{-1}$)**	**References**
Mesoporous MnO_2 nanowire array	Dual-templating method	CP	/	[2]
Hierarchical Mesoporous MnO_2	Soft-interface approach	CP	219	[3]
3D network mesoporous MnO_2	Redox reaction (ambient conditions)	CP	199	[4]
Mesoporous MnO_2 nanosphere	Soft template method	CP	429	[5]
Porous MnO_2	Electrodeposition	CP	/	[6]
Tremella-like MnO_2	Hydrothermal method	CP	93	[7]
Ultrathin MnO_2 nanosheets arrays	Hydrothermal method	CP	237	[8]
Porous MnO_2 tubular arrays	Hydrothermal + template method	CP	/	[9]
Hierarchical mesoporous MnO_2	Redox reaction (ambient conditions)	CP	206	[10]
Porous MnO_2 nanobelts	Hydrothermal +thermal decomposition	SP	/	[11]
Mesoporous MnO_2 nanosheet arrays	Electrodeposition + annealing	SP	/	[12]
Mesoporous MnO_2 nanosheets	In-situ redox reaction (ambient conditions)	SP	288	Our work

[a] Pores are generally classified into two types based on their physical structure, structural pore (SP) and constructed pore (CP).

[b] The specific surface area was calculated from the adsorption data of the N_2 adsorption-desorption isotherm at the relative pressure range of 0.05-0.20.

References

1. K. Kai, Y. Yoshida, H. Kageyama, G. Saito, T. Ishigaki, Y. Furukawa and J. Kawamata, *J. Am. Chem. Soc.*, 2008, **130**, 15938.
2. C. L. Xu, Y. Q. Zhao, G. W. Yang, F. S. Li and H. L. Li, *Chem. Commun.*, 2009, **48**, 7575.
3. Y. Y. Liu, Z. W. Chen, C.−H. Shek, C. M. L. Wu and J. K. L. Lai, *ACS Appl. Mater. Inter.*, 2014, **6**, 9776.
4. J. J. Zhu, L. L. Yu and J. T. Zhao, *J. Power Sources*, 2014, **270**, 411.
5. H. C. Lu, X. Yang, Q. L. Zhao, J. Huang, S. G. Xu, S. K. Cao and Z. Ma, *J. Polym. Sci., Part A: Polym. Chem.*, 2012, **50**, 3641.
6. J. Yang, L. F. Lian, H. C. Ruan, F. Y. Xie and M. D. Wei, *Electrochim. Acta*, 2014, **136**, 189.
7. Y. Y. Ma, R. F. Wang, H. Wang, J. L. Key and S. Ji, *J. Power Sources*, 2015, **280**, 526.
8. M. Hang, X. L. Zhao, F. Li, L. L. Zhang and Y. X. Zhang, *J. Power Sources*, 2015, **277**, 36.
9. F. Li, Y. X. Zhang, M. Huang, Y. Xing and L. L. Zhang, *Electrochim. Acta*, 2015, **154**, 329.
10. S. Bag and C. R. Raj, *J. Mater. Chem. A*, 2016, **4**, 587.
11. J. X. Zhu, W. H. Shi, N. Xiao, X. H. Rui, H. T. Tan, X. H. Lu, H. H. Hng, J. Ma and Q. Y. Yan, *ACS Appl. Mater. Inter.*, 2012, **4**, 2769.
12. M. Kundu and L. Liu, *J. Power Sources*, 2013, **243**, 676.